

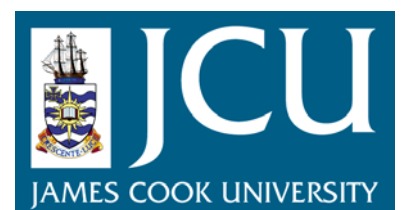
# JCU ePrints

This file is part of the following reference:

**Young, Ian Robert (1983) *The response of waves to an opposing wind*. PhD thesis, James Cook University.**

Access to this file is available from:

<http://eprints.jcu.edu.au/12010>



APPENDIX ADYNAMIC RESPONSE OF PRESSURE TUBING

Bergh and Tijdeman (6) have analysed the motion of a fluid in a tube with a circular cross-section, the fundamental flow equations being the Navier-Stokes equations, the equation of continuity, the equation of state and the energy equation. By assuming that: all disturbances are sinusoidal and very small, the internal radius of the tube is small in comparison with its length and the flow is laminar throughout the system, the above equations can be simplified greatly. Upon applying suitable boundary conditions, the governing equations can then be solved. Bergh and Tijdeman have done this for a series connection of N tubes and N volumes (see Figure A.1), obtaining a recursion formula that relates the sinusoidal pressure disturbance in volume j to the sinusoidal pressure disturbances in the preceding volume j - 1 and the next volume j + 1.

$$\begin{aligned} \frac{P_j}{P_{j-1}} &= \left[ \cosh(\sigma_j L_j) + \frac{V_{vj}}{V_{tj}} \left( \sigma_j + \frac{1}{k_j} \right) n_j \phi_j L_j \sinh(\phi_j L_j) \right. \\ &+ \frac{V_{tj+1} \phi_{j+1} L_j J_0(\alpha_j) J_2(\alpha_{j+1})}{V_{tj} \phi_j L_{j+1} J_0(\alpha_{j+1}) J_2(\alpha_j)} \cdot \frac{\sinh(\phi_j L_j)}{\sinh(\phi_{j+1} L_{j+1})} \\ &\left. \left\{ \cosh(\phi_{j+1} L_{j+1}) - \frac{P_{j+1}}{P_j} \right\} \right]^{-1} \end{aligned} \quad (\text{A.1})$$

where

$$\phi_j = \frac{\omega}{a_{oj}} \left( \frac{J_0(\alpha_j)}{J_2(\alpha_j)} \cdot \frac{\gamma}{n_j} \right)^{\frac{1}{2}} \quad (\text{A.2})$$

$$\alpha_j = i\sqrt{i} R_j \left( \frac{\rho_{sj} \omega}{\mu_j} \right)^{\frac{1}{2}} \quad (\text{A.3})$$

$$n_j = \left[ 1 + \frac{\gamma-1}{\gamma} \frac{J_2(\alpha_j \sqrt{Pr})}{J_0(\alpha_j \sqrt{Pr})} \right]^{-1} \quad (\text{A.4})$$

The quantities are:

$a_o$  = mean velocity of sound

$i$  =  $\sqrt{-1}$

$J_n$  = Bessel function of first kind of order  $n$

$k$  = polytropic constant for the volumes

$L$  = tube length

$p$  = amplitude of pressure disturbance

$R$  = tube radius

$V_v$  = pressure transducer volume

$V_t$  = tube volume

$\mu$  = dynamic viscosity of fluid

$\omega$  = frequency

$\rho_s$  = mean density

$\sigma$  = dimensionless increase in transducer volume due to diaphragm deflection.

From Equation A.1, the expressions for the complex ratio of the pressure fluctuations in each transducer  $j$  to the sinusoidal input pressure  $p_o$  can be obtained by successively putting  $j = N, n-1, \dots, 2, 1$ .

APPENDIX BERROR SOURCES IN SPECTRAL ANALYSIS

The autospectral density function (also called the power spectral density function or variance spectral function) of random data describes the general frequency composition of the data in terms of the spectral density of its mean value. A variance expression for spectral density estimates is most conveniently obtained by direct Fourier transform operations, where the autospectral density function of a stationary (ergodic) Gaussian random process  $x(t)$  is given by

$$E_{xx}(f) = \lim_{T \rightarrow \infty} \frac{2}{T} E [ |X(f,T)|^2 ] \quad (B.1)$$

where  $E[ ]$  indicates the expected value and  $X(f,T)$  is the finite Fourier transform of  $x(t)$ , that is

$$X(f,T) = \int_0^T x(t) e^{-i2\pi ft} dt \quad (B.2)$$

An estimate of  $E_{xx}(f)$  can be obtained by simply omitting the limit and expectation operations in Equation B.1, yielding

$$\hat{E}_{xx}(f) = \frac{2}{T} |X(f,T)|^2 \quad (B.3)$$

In a similar manner, the cross-spectral density function between two time series  $x(t)$  and  $y(t)$  is

$$\hat{E}_{xy}(f) = \frac{2}{T} |X(f,T)| |Y(f,T)| \quad (B.4)$$

The simplifications used to arrive at Equation B.3 introduce possible errors and it can be shown (5) that each frequency component of the estimate  $\hat{E}_{xx}(f)$  will have a sampling distribution given by

$$\frac{\hat{E}_{xx}(f)}{E_{xx}(f)} = \frac{\chi_2^2}{2} \quad (B.5)$$

where  $\chi_2^2$  is the chi-square variable with two degrees of freedom,  $n = 2$ .

Increasing the record length does not alter the distribution function defining the random error of the estimate; it only increases the number of spectral components in the estimate. If the record length is interpreted as a measure of the sample size for the estimate, this implies that Equation B.3 produces an inconsistent estimate of the autospectral density function. The random portion of the estimation error is called the normal standard error

$$\epsilon_r = \sqrt{\frac{2}{n}} \quad (\text{B.6})$$

For the present case,  $n = 2$  and  $\epsilon_r = 1$ , and the standard deviation of the estimate is as large as the quantity being estimated. This would be an unacceptable random error for most applications but it is not uncommon to see raw spectral estimates from Equation B.3 presented as reliable autospectra.

An alternative to presenting the error in terms of  $\epsilon_r$  is to define confidence limits as discussed in Appendix H. Whichever definition of the error is used, it can be reduced in magnitude by increasing the number of degrees of freedom,  $n$ , in the spectral estimate. This can be achieved by smoothing the estimate in one of two ways. The first way is to smooth over an ensemble of estimates by computing individual estimates from  $q$  independent sample records,  $x_i(t)$ ;  $i = 1, 2, \dots, q$ , and then averaging the  $q$  estimates at each frequency of a spectral component. The second way is to smooth over frequency by averaging together  $m$  points either side of a spectral estimate and replacing the original value by this average. If the original frequency resolution was  $\Delta f$ , the resolution after smoothing is  $2m\Delta f$ . There is a similar reduction in frequency resolution for ensemble averaging and is the penalty which must be paid to increase the reliability of the spectral estimate. With ensemble averaging, the number of degrees of freedom becomes  $n = 2q$ , whereas  $n = 2(m+1)$  for frequency averaging. In the present research at least one of these averaging techniques and often both have been used for the spectra presented.

An additional effect which should be considered in spectral calculations is leakage, in which energy is transferred from its correct frequency to a neighbouring frequency as a result of the finite length of the record. Thus,

energy can "leak out" of a spectral bandwidth to bias the spectral estimate downwards or it can "leak in" so that the spectral estimate can be distorted upwards (or downwards if the leakage occurs with negative weighting).

A finite time series can be obtained by passing the infinite time series through a window of finite length. The Fourier transform of the finite series becomes

$$X(f) = Y(f) U_T(f) \quad (\text{B.7})$$

where  $Y(f)$  and  $U(f)$  are the Fourier transforms of the infinite time series and the window respectively. If the time series is simply truncated, the window function is called a boxcar window, its Fourier transform being presented in Figure B.1. To reduce this leakage problem, it is necessary to modify the boxcar type of weighting in the time domain (or its equivalent Fourier transform operations in the frequency domain) so as to broaden the main lobe and decrease the side lobes shown in Figure B.1. A number of different window functions which reduce the leakage have been proposed, the most popular being the Hanning window (10) and the one-tenth cosine taper window (9). The Hanning window has the form of a full cosine bell and is given by

$$u_T(t) = \frac{1}{2} \left( 1 + \cos \frac{2\pi t}{T} \right), \quad -\frac{T}{2} \leq t \leq \frac{T}{2} \quad (\text{B.8})$$

whereas the one-tenth cosine taper is defined by

$$u_T(t) = \begin{cases} \cos \frac{5\pi t}{T}, & -\frac{T}{2} \leq t < -\frac{2T}{5} \\ 1, & -\frac{2T}{5} \leq t < \frac{2T}{5} \\ \cos \frac{5\pi t}{T}, & \frac{2T}{5} \leq t < \frac{T}{2} \end{cases} \quad (\text{B.9})$$

The Fourier transform of these two window shapes are shown in Figure B.1 for comparison with the boxcar window. The reduction in the magnitude of the side lobes for the two tapered windows is quite apparent. All spectral analysis in this project has utilized the one-tenth cosine taper window.

APPENDIX CANALYSIS OF VERY NARROW BAND DATA

In determining the energy flux between wind and waves, the two critical quantities which must be determined are the magnitude of the surface stress and its phase relative to the surface waves. The techniques of auto and cross spectral analysis are ideally suited to determining these quantities from time series of surface stress and water level elevation. Indeed, many previous investigators have relied extensively upon such techniques (117, 134). In this research the waves generated by the wave maker were invariably sinusoidal and therefore distinctly narrow banded. The theoretical autospectrum of a sine wave of frequency  $f$  is a spike of infinite height located at  $f$ . In practice, this result is distorted by the discrete finite record length. An approximate definition for the autospectrum was given by Equation B.3. It can be more rigorously defined by

$$E_{xx}(f) = \lim_{\Delta f \rightarrow 0} \frac{1}{\Delta f} \left[ \lim_{T \rightarrow \infty} \frac{1}{T} \int_0^T x^2(t, f, \Delta f) dt \right] \quad (C.1)$$

When spectra are calculated using the Fourier transform technique,  $\Delta f = 1/T$ , so that, for a finite length record, limiting processes in Equation C.1 are violated. This is true for spectral estimates of any time series, not just narrow band records. The finite frequency resolution, however, means that it is highly probable that the frequency  $f$  will not coincide with one of the frequencies of a calculated spectral value,  $m\Delta f$ . The final result is a broader finite height spike rather than an infinite spike. This distortion becomes progressively worse as the length of the time series is reduced. Therefore, the calculated spectral shape is dependent upon the record length and also on how closely the sine wave frequency corresponds to a discrete calculation frequency. The effects of the finite record length can be seen in Figure C.1. This figure shows calculated spectra for a sinusoid with  $f = 0.1$  Hz but varying record lengths of 136.5, 68.3, 34.1, 17.1, 8.5 and 4.3 mins. Such strong dependence on the sampling parameters is obviously unacceptable and indicates an alternative technique is required for reliably analysing such narrow banded records.

An alternative approach is available in the time domain, where the equivalents of the auto and cross-spectral functions are the autocorrelation and crosscorrelation functions. The autocorrelation function of random data describes the general dependence of the values of the data at one time on the values at another time. An estimate for the autocorrelation between the values of  $x(t)$  and times  $t$  and  $t + \tau$  may be obtained by taking the product of the two values and averaging over the observation time  $T$ . The resulting average product will approach an exact autocorrelation function as  $T$  approaches infinity:

$$R_x(\tau) = \lim_{T \rightarrow \infty} \frac{1}{T} \int_0^T x(t) x(t + \tau) dt \quad (C.2)$$

Provided the mean of  $x(t)$  is zero,  $R_x(0) = \sigma^2$ , the variance of the record.

For a sinusoidal time series  $x(t) = a \sin \omega t$ ,

$$R_x(\tau) = \frac{a^2}{2} \cos \omega \tau \quad (C.3)$$

Therefore, the autocorrelogram will persist periodically over all time displacements with an amplitude equal to the original sine wave variance and a period equal to that of the original sine wave. All phase information is lost however.

The crosscorrelation function can be defined in a similar manner to Equation C.2 as

$$R_{xy}(\tau) = \lim_{T \rightarrow \infty} \frac{1}{T} \int_0^T x(t) y(t + \tau) dt \quad (C.4)$$

For the case of two sinusoidal signals with a phase difference  $\phi$ ,  $x(t) = a \sin \omega t$  and  $y(t) = b \sin (\omega t + \phi)$ , the cross correlation is

$$R_{xy}(\tau) = a b \cos (\omega \tau - \phi) \quad (C.5)$$

The crosscorrelogram is again periodic with maxima at values of  $\tau$  such that

$$2\pi \frac{T}{T} = \phi + 2n\pi \quad (\text{C.6})$$

where  $T$  is the period of the sine wave and  $n$  is an integer. This behaviour is illustrated in Figure C.2.

In summary, for very narrow band data, the amplitude and frequency of the signal can be obtained from the autocorrelogram and the phase relationship between the two signals from the crosscorrelogram. This correlogram technique has been used in preference to the spectral approach throughout this research.

APPENDIX DCORRECTIONS FOR SYSTEM RESPONSE

In Chapter 4 the response of all the individual systems was examined and transfer functions obtained. To obtain accurate results it is necessary to correct recorded time series for the effects of these system responses. For a system with an input  $x(t)$  and an output  $y(t)$ , Equation 3.30 showed that their Fourier transforms are related as

$$Y(f) = H(f) X(f) \quad (D.1)$$

In the discrete finite case, the Fourier transform pair are

$$X(r) = \frac{T}{N} \sum_{k=0}^{N-1} x_k \exp \frac{-i2\pi rk}{N} \quad (D.2)$$

$$r = 0, 1, \dots, N-1$$

and

$$x_k = \frac{1}{T} \sum_{r=0}^{N-1} X(r) \exp \frac{i2\pi rk}{N} \quad (D.3)$$

$$k = 0, 1, \dots, N-1$$

The simple procedure for correcting for the transfer function is then:

- (a) Determine  $Y(f)$  from the output  $y(t)$  and Equation D.2
- (b) Divide  $Y(f)$  by  $H(f)$  to obtain  $X(f)$
- (c) Determine  $x(t)$  from  $X(f)$  and Equation D.3.

The procedure is complicated, however, by the fact that Fast Fourier Transform (FFT) algorithms only define the transform in the range  $r = 0, 1, \dots, N/2$ . Therefore it is necessary to determine the remaining Fourier coefficients before the inverse transform procedure can be applied. These can be found from the relationships (5)

$$\operatorname{Re}\{X(r)\} = \operatorname{Re}\{X(N-r)\} \quad (\text{D.4})$$

$$\text{and } \operatorname{Im}\{X(r)\} = -\operatorname{Im}\{X(N-r)\} \quad (\text{D.5})$$

To preserve symmetry, the imaginary part of  $X(N/2)$  is set to zero as illustrated in Figure D.1. The discrete Fourier Transform is thus defined over the range  $X(0), X(1), \dots, X(N-1)$  and the previously outlined procedure for correcting for the effects of system response can be applied.

In addition, if the input to a system  $x(t)$  is known, the output  $y(t)$  can be found in a similar manner. The only difference is that the Fourier transform of  $x(t)$  is multiplied by  $H(f)$  rather than being divided. The analysis procedure described in this appendix and the computer programs which implement it can be checked in the following manner. For an arbitrary input to and transfer function for a system the corresponding output can be found. The reverse procedure can then be run. The final result should be identical with the initial input. Such a test was conducted and the results appear in Figure D.2. The time series illustrated in this figure clearly show that both the correction technique and the computer programs which implement it are performing satisfactorily.

APPENDIX EANALYSIS OF PRESSURE DATA

The ultimate goal of the pressure measurements described in Chapter 7 was to determine the magnitude and phase of the wave-induced air pressure relative to the surface waves. The quantities measured were the water surface elevation, the differential pressure between the disk and total probes,  $\Delta p_{Dt} = p_D - p_t$  and the differential pressure between the disk probe and the free stream static probe,  $\Delta p_{Ds} = p_D - p_{so}$ . The analysis of these signals to determine the wave-induced static pressure,  $p_s - p_{so}$ , was complicated by the frequency response characteristics of the measurement system, shown schematically in Figure E.1. Specific influences include: probe calibration, wave follower oscillation pressures, dynamic response of the pressure tubing, pressure transducer calibration and response, low pass filter characteristics and D.C. amplifier response.

The full analysis procedure consisted of nine sequential steps which are described below

- (1) The analog time series for water surface elevation,  $\eta$ , disk-total differential pressure,  $\Delta p_{Dt}$  and disk-static differential pressure,  $\Delta p_{Ds}$  were converted to physical units using the appropriate wave gauge and pressure transducer calibration curves. The pressure readings were also corrected for the particular gain used for the D.C. amplifiers.
- (2) The differential pressure signals were corrected for the effects of the 5 Hz low pass filters using the analysis technique described in Appendix D. The filter transfer functions, as shown in Figure 4.28, were assumed to have  $|H| = 1$  and  $\phi = 0^\circ$  for frequencies above 5 Hz. Had this assumption not been made, then the high frequency noise (above 5 Hz) which the filter was used to remove would have been regenerated by the filter transfer function correction process.
- (3) The pressures created by the motion of the wave follower were calculated assuming the input to the system was the water surface elevation. This assumes that the wave follower motion and the water surface

elevation are identical, shown in Section 4.2.2 to be a reasonable assumption. This step represents the reverse process to step (2). Here, the input to the system is known and the output is required, whereas in (2) the output was known and the input had to be determined.

- (4) The wave follower oscillation pressures, calculated in step (3) were subtracted from the differential pressures of step (2).
- (5) The resulting differential pressure signals of step (4) were corrected for the dynamic response of the thin pressure tubes. Although the transfer functions for each individual tube are known, it is the effects on the differential measurements which must be considered. Therefore, the two sides of the differential measurement will be effected independently by the response of the tubes. The effect on the differential measurement is complicated and its calculation is discussed later. The resulting differential pressures at the end of this stage were the actual pressures sensed by the probes,  $\Delta p_{Ds}$  and  $\Delta p_{Dt}$ , and were free from the effects of instrumentation response.
- (6) The water surface elevation and differential pressure signals were filtered using a non-recursive digital low pass filter (see Appendix J) to remove harmonics of the primary frequency. The cut-off frequency of the filter was chosen such that it lay between the first and second harmonics.
- (7) Using the filtered differential pressure measurements, together with the disk-probe calibration of Section 4.3.3,  $p_s - p_{s0}$  was determined as outlined in Section 4.3.1. This value represents the required wave-induced static pressure.
- (8) The autocorrelograms of  $\eta$  and  $p_s - p_{s0}$  were calculated together with the crosscorrelogram of the two signals.
- (9) Using the technique for analysing very narrow band data outlined in Appendix C, the frequency and amplitudes were determined from the autocorrelograms and the phase difference from the crosscorrelogram.

As mentioned earlier the correction of the pressure signals for the dynamic effects of the thin pressure tubes posed problems. Although the transfer functions for the four individual tubes were determined in Section 4.3.6, the output signal for each tube was not known, only the differential outputs being recorded. It was these differential outputs which needed to be corrected to determine the actual differential inputs.

The applied and measured pressures are shown in Figure E.2 together with the individual tube transfer functions. The applied pressures are the total pressure  $p_t(\omega)$ , the disk pressure  $p_D(\omega)$  and the free stream static pressure  $p_{s0}$ . The corresponding measured output pressures are  $P_t(\omega)$ ,  $P_{D1}(\omega)$  or  $P_{D2}(\omega)$  and  $P_s$ . There are two output pressures for the disk as it is connected to the positive parts of both transducers. All the pressures are expressed as functions of the cyclic frequency  $\omega$ , except the free stream static pressure which is a constant. The tube transfer functions are identified as:  $H_t(\omega)$  for the total line,  $H_{D1}(\omega)$  for the disk to transducer 1 line,  $H_{D2}(\omega)$  for the disk transducer 2 line and  $H_s(\omega)$  for the static line.

Since  $p_s$  is a constant and  $H_s(0) = 1.0$

$$P_s = P_s \quad (E.1)$$

Also, since  $H_{D2}(0) = 1.0$

$$F[P_D(\omega) - p_s] = F[P_{D2}(\omega) - P_s] / H_{D2}(\omega) \quad (E.2)$$

where the notation  $F[ ]$  indicates the Fourier transform of  $[ ]$ . Finding the inverse Fourier transform of the left hand side of Equation E.2 gives  $p_D(\omega) - p_s$  which is one of the required differential inputs. Now that  $p_D(\omega) - p_s$  is known and again since  $H_{D1}(0) = 1.0$ , it follows that

$$F[P_{D1}(\omega) - p_s] = F[p_D(\omega) - p_s] H_{D1}(\omega) \quad (E.3)$$

which upon finding the inverse Fourier transform yields  $P_{D1}(\omega) - p_s$ .  
Therefore

$$P_t(\omega) - p_s = [P_{D_1}(\omega) - p_s] - [P_{D_1}(\omega) - P_t(\omega)] \quad (E.4)$$

which is calculable since  $P_{D_1}(\omega) - P_t(\omega)$  is the quantity being measured by transducer 1. Proceeding in a similar manner gives

$$F[P_t(\omega) - p_s] = F[P_t(\omega) - p_s] / H_t(\omega) \quad (E.5)$$

which yields  $p_t(\omega) - p_s$ . Finally then

$$P_D(\omega) - p_t(\omega) = [P_D(\omega) - p_s] - [p_t(\omega) - p_s] \quad (E.6)$$

where  $p_t(\omega) - p_s$  is known from above and  $p_D(\omega) - p_s$  was calculated earlier. Thus  $p_D(\omega) - p_t(\omega)$  represents the second differential input and the measured differential values have been corrected for the effects of the pressure tubing.

Because of the considerable numerical manipulation involved in the above correction process, a test procedure was devised to confirm the successful operation of the computer program which performed this process. The details of this test and its results are shown in Appendix F.

APPENDIX FTEST PROCEDURE FOR COMPUTER PROGRAM FOR TRANSFER FUNCTION CORRECTION OF DIFFERENTIAL PRESSURE RECORDS

In describing the procedure used to test the computer program TUBTRN.FOR, which corrected the differential pressure measurements for the finite response of the pressure tubing, the same terminology described in Appendix E and Figure E.2 is adopted. The test followed five individual steps:

- (1) Synthetic input signals  $p_s$ ,  $p_D(\omega)$  and  $p_t(\omega)$  were generated.
- (2) Using the standard single channel transfer function correction program RTRNFR.FOR the corresponding output pressures were determined for each tube:  $P_s$ ,  $P_{D_1}(\omega)$ ,  $P_{D_2}(\omega)$  and  $P_t(\omega)$ .
- (3) The output differential pressures were determined

$$\Delta P_1(\omega) = P_{D_1}(\omega) - P_t(\omega) \quad (F.1)$$

$$\text{and } \Delta P_2(\omega) = P_{D_2}(\omega) - P_s \quad (F.2)$$

- (4) TUBTRN.FOR was used to process  $\Delta P_1(\omega)$  and  $\Delta P_2(\omega)$  to determine the corresponding input differential pressures  $\Delta p_1(\omega)$  and  $\Delta p_2(\omega)$ .
- (5) If TUBTRN.FOR was performed correctly

$$\Delta p_1(\omega) = p_D(\omega) - p_t(\omega) \quad (F.3)$$

$$\text{and } \Delta p_2(\omega) = p_D(\omega) - p_s \quad (F.4)$$

The results of the test are shown in Figure F.1 and clearly illustrate that the relations defined by Equations F.3 and F.4 are satisfied. Thus it can be concluded that the program TUBTRN.FOR was performing correctly.

APPENDIX GANALYSIS OF VELOCITY DATA

The aim of the velocity measurements described in Chapter 8 was to use the data from a cross hot film probe to determine the horizontal and vertical components of the velocity field. From these velocity measurements both the structure of the air flow above the waves and the Reynolds stresses can be determined. This velocity data was acquired in two separate fashions, by the minicomputer and by the spectrum analyser.

(a) Data Acquired with Minicomputer

The velocity data was considerably easier to analyse than the pressure data since there were fewer intermediate systems which could distort the signal. In fact, the only intermediate devices which needed to be considered were the wave follower and the low pass anti-aliasing filters. The full system is shown schematically in Figure G.1.

The full analysis procedure was as follows.

- (1) The two cross film signals and the water surface elevation signals were converted from analog values to physical units using the appropriate calibration data. Particular care was taken to correct the cross film calibration curves for temperature drift before the time series were reduced.
- (2) The cross film signals were then corrected for the effects of the analog low pass anti-aliasing filters.
- (3) Since the cross film probes were aligned at  $\pm 45^\circ$  to the x airflow direction, it can be shown that the cooling velocities for the probes were  $(u-w)/\sqrt{2}$  and  $(u+w)/\sqrt{2}$  respectively. Therefore, with these two records, it was a simple matter to determine u and w by simultaneous solution.

- (4) Some velocity data was obtained using stationary probes but most was recorded using the wave follower in a moving frame of reference. In this case there was no need to subtract any effects due to the oscillatory motion of the wave follower as was done for the pressure data. The  $w$  time series will have a component equal to the vertical velocity of the water surface,  $\partial\eta/\partial t$ . This is a true velocity sensed in the moving frame of reference and bears no similarity to the acceleration effects of the pressure data. The effects of the hunting motion of the wave follower were removed using a digital band-reject filter (see Appendix J) with cut-off frequencies at 15 Hz and 17 Hz.
- (5) At this stage corrected time series of the horizontal and vertical velocity components,  $u = \bar{u} + \tilde{u} + u'$  and  $w = \bar{w} + \tilde{w} + w'$  had been obtained and it only remained necessary to determine the stresses from these time series. The mean values  $\bar{u}$  and  $\bar{w}$  were firstly subtracted from the two time series and the wave-induced components  $\tilde{u}$  and  $\tilde{w}$  were obtained using a digital band-pass filter (see Appendix J). The mean values were subtracted from the original time series to obtain the oscillatory components of velocity,  $u'' = \tilde{u} + u'$  and  $w'' = \tilde{w} + w'$ . Using these components, the product terms  $u''w''$ ,  $u''u''$  and  $w''w''$  were obtained. Taking the means of these three records yielded the Reynolds stresses  $\overline{u''w''}$ ,  $\overline{u''u''}$  and  $\overline{w''w''}$ , whereas band-pass filtering yielded the wave-induced momentum flux terms  $\widetilde{u''w''}$ ,  $\widetilde{u''u''}$  and  $\widetilde{w''w''}$ .
- (6) The variances of  $\eta$ ,  $\tilde{u}$ ,  $\tilde{w}$ ,  $u''w''$ ,  $u''u''$  and  $w''w''$  were found and hence the amplitudes of the records.
- (7) The cross correlograms between  $\eta$  and the five wave-induced components were found, and from these the phase relationships determined.
- (b) Data Acquired with Spectrum Analyser

The data analysis technique used with the spectrum analyser was quite simple as most of the process was performed by hardware. The outputs from the hot film anemometer were passed through a linearizing circuit to produce outputs directly proportional to  $u + w$  and  $u - w$ . These signals were then passed through a sum and difference circuit to produce outputs proportional to  $u$  and  $w$ . The linearizing, sum and difference circuits were all built

into the I.S.V.R. hot film anemometer. These signals were then suitable for direct input to the spectrum analyser. The spectrum analyser removed the means from the signals and evaluated spectra of  $u''$  and  $w''$  as well as the coherence function and phase relationship between  $u''$  and  $w''$ . The spectra were determined over two frequency ranges, 0 to 10 Hz and 0 to 2500 Hz. To ensure statistical significance for these spectral estimates (see Appendix B), a number of individual spectra were averaged to produce the final result. For the low frequency range 32 spectra were averaged, whereas for the high frequency range 128 spectra were averaged.

The output from the spectrum analyser was plotted on a Rikadenki Model BW-132 X, Y plotter and these plots were later digitised using a Summagraphics digitising table. The digital data was then transferred to the DEC-SYSTEM 1091 mainframe computer for storage.

APPENDIX HERROR ANALYSIS

In the interpretation of the results of any experiment the question "How reliable are these results?" must ultimately be asked. It is inevitable that, even in the most carefully conducted experiments, some errors will occur. Consequently, it is necessary to estimate the possible magnitude of such errors and to present these error estimates along with the experimental data.

(a) Types of Errors and their Propagation

There are four basic types of errors which can occur in an experiment; accidental errors, fixed errors, mistakes and statistical errors. Accidental errors are those varying errors which cause repeated readings to differ without apparent reason. Accidental errors arise from instrument friction and lag time, personal errors and many other causes. Fixed errors are those which cause repeated readings to be in error by the same amount without apparent reason. (If a reason were known, presumably a suitable correction could be made and the error eliminated). Fixed errors arise from such causes as a burr on the lip of a Pitot tube or an incorrect calibration relationship. Mistakes are completely erroneous readings of scales, transducers and so on. Statistical errors arise when some property of a population is estimated from a finite sample of values. An example is the estimation of the mean wind velocity from a wind record of limited duration.

There are a number of different ways in which to represent the estimated error for some experimentally determined quantity. The most convenient method is to use confidence limits. If it is assumed that the errors follow some known probability distribution, it is possible to define upper and lower limits between which the true value will have a known probability of occurring. Therefore, if these limits  $a$  and  $b$  are chosen such that the probability of the true value occurring between them is 0.95, then the interval between  $a$  and  $b$  is described as a 95% confidence interval. In other words, the computed interval can be assumed to contain the true parameter with 95% confidence. Hence some experimentally determined

parameter  $x$  can be expressed as  $x \pm \epsilon$  with  $(1 - \alpha)100\%$  confidence that the true value of  $x$  lies between  $x - \epsilon$  and  $x + \epsilon$ . Because of the nature of the probability distributions of the errors, the longer the confidence interval the higher the confidence that the given interval contains the unknown parameter. A 100% confidence can, however, never be obtained unless the confidence interval is infinite.

In addition to estimating the errors for measured quantities, it is important to determine how such errors will effect a result which is a function of a number of measured quantities. Kline and McClintock (63) have proposed a procedure to determine the uncertainty  $\delta R$  in a general dependent quantity  $R(x_i)$  as

$$\delta R = \pm \left[ \sum_{i=1}^n \left( \frac{\partial R}{\partial x_i} \delta x_i \right)^2 \right]^{1/2} \quad (\text{H.1})$$

where  $x_i$  are the measured quantities upon which  $R$  is dependent. Thus, using Equation H.1 it is possible to determine the errors for values which are derived from a number of measured quantities.

(b) Statistical Errors

(i) Mean Values

Walpole and Myers (132) have shown that the  $(1 - \alpha)100\%$  confidence interval for the mean of a population  $\bar{\mu}$  is

$$\bar{x} - Z_{\alpha/2} \frac{\sigma}{\sqrt{n}} < \bar{\mu} < \bar{x} + Z_{\alpha/2} \frac{\sigma}{\sqrt{n}} \quad (\text{H.2})$$

where  $\bar{x}$  is the mean of a sample of size  $n$  from a population with known variance  $\sigma^2$  and  $Z_{\alpha/2}$  is the value of the standard normal distribution leaving an area of  $\alpha/2$  to the right. To use Equation H.2 it is necessary to know the standard deviation of the population,  $\sigma$ . This quantity is generally not known. If  $n \geq 30$ , however,  $\sigma$  can be replaced by  $S$ , the standard deviation of the sample, with little error.

(ii) Variance

The  $(1 - \alpha)$  100% confidence interval for the variance  $\sigma^2$  of a population is (132)

$$\frac{(n-1) S^2}{\chi_{\nu; \alpha/2}^2} < \sigma^2 < \frac{(n-1) S^2}{\chi_{\nu; 1-\alpha/2}^2} \quad (\text{H.3})$$

where  $S^2$  is the variance of a sample of size  $n$ , and  $\chi_{\nu; \alpha/2}^2$  and  $\chi_{\nu; 1-\alpha/2}^2$  are the values of a chi-square distribution with  $\nu = n-1$  degrees of freedom leaving areas of  $\alpha/2$  and  $1 - \alpha/2$ , respectively, to the right.

Throughout this project the amplitude of sinusoidal signals has been determined from the variance, using the relation  $a = \sqrt{2\sigma^2}$ , where  $a$  is the amplitude. If the error on the variance  $\delta\sigma^2$  is  $\epsilon\sigma^2$  then from Equation H.1

$$\begin{aligned} \delta a &= \frac{\partial a}{\partial \sigma^2} \epsilon \sigma^2 = \frac{\epsilon \sigma^2}{\sqrt{2\sigma^2}} \\ &= a \frac{\epsilon}{2} \end{aligned} \quad (\text{H.4})$$

Therefore, the percentage error on the amplitude is half that of the variance.

(iii) Spectral Estimates

It can be shown (86) that autospectral estimates approximately follow a chi-square distribution with  $n$  degrees of freedom, where

$$n = 2q(2m + 1) \quad (\text{H.5})$$

In Equation H.5 the spectrum is ensemble averaged over  $q$  spectral estimates and frequency averaged over  $2m + 1$  points as described in Appendix B. The confidence interval then becomes

$$\frac{n \hat{E}(f)}{\chi_{n; \alpha/2}^2} < E(f) < \frac{n \hat{E}(f)}{\chi_{n; 1-\alpha/2}^2} \quad (\text{H.6})$$

where  $\hat{E}(f)$  is the spectral estimate of the sample.

(iv) Coherence Function

Bendat and Piersol (5) indicate that empirical studies show that estimates of coherence functions in the range  $0.35 \leq \gamma_{xy}^2(f) \leq 0.95$  based upon spectral density estimates with  $n \geq 40$  degrees of freedom can be evaluated in terms of the transformation

$$w(f) = \frac{1}{2} \ln \frac{1 + \hat{\gamma}_{xy}(f)}{1 - \hat{\gamma}_{xy}(f)} = \tanh^{-1} \hat{\gamma}_{xy}(f) \quad (\text{H.7})$$

$\hat{\gamma}_{xy}(f)$  is the calculated coherence function of the sample and  $w(f)$  has an approximate normal distribution with a mean and variance of

$$\bar{\mu}_x = (n - 2)^{-1} + \tanh^{-1} \gamma_{xy}(f) \quad (\text{H.8})$$

$$\text{and } \sigma_w^2 = (n - 2)^{-1} \quad (\text{H.9})$$

The  $(1 - \alpha)100\%$  confidence interval then becomes

$$\tanh\{w(f) - (n - 2)^{-1} - \sigma_w Z_{\alpha/2}\} < \gamma_{xy}(f) \leq \tanh\{w(f) - (n - 2)^{-1} + \sigma_w Z_{\alpha/2}\} \quad (\text{H.10})$$

The above result gives the  $(1 - \alpha)100\%$  confidence interval for  $\gamma_{xy}(f)$  as a function of  $n$ ,  $\hat{\gamma}_{xy}(f)$  and  $\alpha$ . The confidence limits for  $\gamma_{xy}^2(f)$  are the square of the corresponding limits for  $\gamma_{xy}(f)$ .

(v) Transfer Function

Bendat and Piersol (5) have shown that the  $(1 - \alpha)100\%$  confidence interval for  $H(f)$  can be determined by a quantity  $\hat{F}(f)$  such that

$$|\hat{H}(f) - H(f)|^2 \leq \hat{F}^2(f) \quad (\text{H.11})$$

$$\hat{r}^2(f) = \frac{2}{(n-2)} F_{2,n-2;\alpha} [1 - \hat{\gamma}_{xy}^2(f)] \frac{\hat{E}_{yy}(f)}{\hat{E}_{xx}(f)} \quad (\text{H.12})$$

where  $n$  is the number of degrees of freedom of each spectral estimate,  $F_{2,n-2;\alpha}$  is the  $100\alpha$  percentage point of an F distribution with  $n_1 = 2$  and  $n_2 = n - 2$  degrees of freedom,  $\hat{E}_{xx}(f)$  is the autospectral estimate of the output  $y(t)$  and  $\hat{\gamma}_{xy}^2(f)$  is the sample estimate of the ordinary coherence function between the input  $x(t)$  and the output  $y(t)$ . Geometrically, Equation H.12 describes a circle of radius  $\hat{r}(f)$  centred at  $\hat{H}(f)$ . In terms of the gain estimate  $|\hat{H}(f)|$  and the phase estimate  $\hat{\phi}(f)$ , the approximate confidence intervals for the actual gain  $|H(f)|$  and phase  $\phi(f)$  are given by

$$|\hat{H}(f)| - \hat{r}(f) \leq |H(f)| \leq |\hat{H}(f)| + \hat{r}(f) \quad (\text{H.13a})$$

$$\text{and } \hat{\phi}(f) - \Delta\hat{\phi}(f) \leq \phi(f) \leq \hat{\phi}(f) + \Delta\hat{\phi}(f) \quad (\text{H.13b})$$

where  $\hat{r}(f)$  is the positive square root of  $r(f)$  and

$$\Delta\hat{\phi}(f) = \sin^{-1} \frac{\hat{r}(f)}{|\hat{H}(f)|} \quad (\text{H.14})$$

#### (vi) Phase Measurements

The phase difference between various quantities was determined from the crosscorrelogram as described in Appendix C. The phase angle  $\phi$  is given by  $\phi = 360 t_{\text{lag}}/T$  where  $t_{\text{lag}}$  is the lag time at which the crosscorrelogram is a maximum. Since the sampling interval was  $\Delta t$  the possible error on  $t_{\text{lag}}$ ,  $\Delta t_{\text{lag}} = \Delta t/2 = 1/120$  s.

Applying Equation H.1 gives

$$\Delta\phi = 3f \quad (\text{H.15})$$

Therefore the possible phase error increases with increasing frequency.

(c) Error Propagation for Specific Quantities(i) Transfer Functions from Sinusoidal Inputs

As well as determining transfer functions from spectral quantities, they were also evaluated from sinusoidal inputs. The gain of the transfer function is  $|H| = b/a$ , where  $a$  and  $b$  are the amplitudes of the input and output signals, respectively. If the percentage error in  $a$  and  $b$  is  $\epsilon$ , Equation H.1 yields

$$\Delta|H| = \sqrt{2} \epsilon b/a \quad (\text{H.16})$$

Therefore, the percentage error in the transfer function is  $\sqrt{2}\epsilon$ .

(ii) Potential Flow Functions

In the analysis of the recorded data it was necessary to evaluate three functions derived from potential flow theory for the wave-induced pressure and velocity. These functions include the pressure function  $R_1 = ae^{-kz}(1 - U/C)^2$ , the non-dimensional velocity function  $R_2 = a/U(\omega - kU)e^{-kz}$  and the squared velocity function  $R_3 = [a(\omega - kU)e^{-kz}]^2$ . If it is assumed that the errors in the measured quantities  $a$ ,  $z$  and  $U$  are  $\Delta a = \epsilon_a a$ ,  $\Delta z = \epsilon_z z$  and  $\Delta U = \epsilon_U U$ , Equation H.1 yields

$$\Delta R_1 = R_1 \left\{ \epsilon_a^2 + (\epsilon_z kz)^2 + 4 \left[ \frac{\epsilon_U U}{C(1 - U/C)} \right]^2 \right\}^{1/2} \quad (\text{H.17})$$

$$\Delta R_2 = R_2 \left\{ \epsilon_a^2 + (\epsilon_z kz)^2 + \left[ \frac{\epsilon_U \omega}{(\omega - kU)} \right]^2 \right\}^{1/2} \quad (\text{H.18})$$

$$\Delta R_3 = R_3 \cdot 2 \left\{ \epsilon_a^2 + (\epsilon_z kz)^2 + \left[ \frac{\epsilon_U kU}{(\omega - kU)} \right]^2 \right\}^{1/2} \quad (\text{H.19})$$

(d) Magnitude of Specific Errors

Using the various results derived in this Appendix, it is possible to assign numerical values to the various measured and derived quantities. These errors are presented in Table H.1 and represent 95% confidence intervals.

The errors generally consist of an accidental error due to the accuracy of calibration results or the precision to which an instrument can be read and statistical errors caused by the finite length of the time series measured.

Quantity	Accidental Error	Source	Statistical Error	Source	Total Error
a	±2%	Calibration	±6%	Eqs. H.3 & H.4	±8%
$\bar{u}$	±5%	Calibration	±1%	Eq. H.2	±6%
$\frac{u''u''}{\bar{u}}$	±10%	Cal. & H.1	±3%	Eq. H.2	±13%
$\frac{w''w''}{\bar{u}}$	±10%	Cal. & H.1	±3%	Eq. H.2	±13%
$\frac{u''u''}{\bar{u}}$	±8%	Cal. & H.1	±7%	Eq. H.2	±15%
amp( $\tilde{u}$ )	±5%	Calibration	±6%	Eqs. H.3 & H.4	±11%
amp( $\tilde{w}$ )	±5%	Calibration	±6%	Eqs. H.3 & H.4	±11%
amp( $\tilde{u}$ )/ $\bar{u}$	±8%	Cal. & H.16	±6%	Eqs. H.3 & H.4	±14%
amp( $\tilde{w}$ )/ $\bar{u}$	±8%	Cal. & H.16	±6%	Eqs. H.3 & H.4	±14%
$\frac{\text{amp}(\tilde{u}) \text{amp}(\tilde{u})}{\bar{u}}$	±10%	H.1 & $\tilde{u}$	±12%	Eq. H.1 & $\tilde{u}$	±22%
$\frac{\text{amp}(\tilde{w}) \text{amp}(\tilde{w})}{\bar{u}}$	±10%	H.1 & $\tilde{w}$	±12%	Eq. H.1 & $\tilde{w}$	±22%
$\frac{\text{amp}(\tilde{u}) \text{amp}(\tilde{w})}{\bar{u}}$	±7%	H.1 & $\tilde{u}$ & $\tilde{w}$	±9%	Eq. H.1 & $\tilde{u}$ & $\tilde{w}$	±16%
$\phi$	-		±6%	$\Delta t$ & H.15	±6%
$\bar{u}^2$	±10%	Cal. & H.1	±2%	Eq. H.1 & H.2	±12%
$R_1$	-		-	Eq. H.17	±12%
$R_2$	-		-	Eq. H.18	±8%
$R_3$	-		-	Eq. H.19	±19%
H	-		-	Eq. H.16 & a	±11%
amp( $\tilde{p}$ )	±3%	Calibration	±6%	Eq. H.3 & H.4	±9%

Table H.1 Estimated experimental errors.

APPENDIX ILEAST SQUARES CURVE FITTING

Throughout this project extensive use has been made of least squares curve approximations to recorded data. Two types of curves were used: polynomial relationships and, for the hot film probe calibration curves, a specific power relationship.

(a) Polynomial Curve Approximations

It is desired to fit a curve of the form

$$y = a_0 + a_1x + a_2x^2 + \dots + a_mx^m \quad (\text{I.1})$$

$$= \sum_{j=0}^m a_j x^j \quad (\text{I.2})$$

to the known data points,  $x_i, y_i, i = 1 \dots n$ . Therefore it is necessary to minimize

$$q = \sum_{i=1}^n \left[ y_i - \sum_{j=0}^m (a_j x_i^j) \right]^2 \quad (\text{I.3})$$

The normal equations which must be solved to minimize Equation I.3 are

$$\frac{\partial q}{\partial a_0} = -2 \sum_{i=1}^n \left[ y_i - \sum_{j=0}^m (a_j x_i^j) \right] = 0 \quad (\text{I.4a})$$

$$\frac{\partial q}{\partial a_1} = -2 \sum_{i=1}^n \left\{ x_i^2 \left[ y_i - \sum_{j=0}^m (a_j x_i^j) \right] \right\} = 0 \quad (\text{I.4b})$$

$$\frac{\partial q}{\partial a_2} = -2 \sum_{i=1}^n \left\{ x_i^4 \left[ y_i - \sum_{j=0}^m (a_j x_i^j) \right] \right\} = 0 \quad (\text{I.4c})$$

·  
·  
·

$$\frac{\partial q}{\partial a_m} = -2 \sum_{i=1}^n \left\{ x_i^m \left[ y_i - \sum_{j=0}^m (a_j x_i^j) \right] \right\} = 0 \quad (\text{I.4d})$$

Equations I.4 represent a system of  $m + 1$  linear simultaneous equations in the unknowns  $a_0 \dots a_m$ . Since the equations are linear, their solution is quite simple.

(b) Hot Film Curve Approximation

To approximate the hot film calibration curves, it was desired to fit a curve of the form

$$y = a + bx^c \quad (I.5)$$

to the measured data points  $x_i, y_i, i = 1 \dots n$ . Therefore, it is required to minimize

$$q = \sum_{i=1}^n (y_i - a - bx_i^c)^2 \quad (I.6)$$

for which the normal equations become

$$\frac{\partial q}{\partial a} = -2 \sum_{i=1}^n (y_i - a - bx_i^c) = 0 \quad (I.7a)$$

$$\frac{\partial q}{\partial b} = -2 \sum_{i=1}^n [x_i^c (y_i - a - bx_i^c)] = 0 \quad (I.7b)$$

$$\frac{\partial q}{\partial c} = -2 \sum_{i=1}^n [(b x_i^c \ln x_i) (y_i - a - bx_i^c)] = 0 \quad (I.7c)$$

Equations I.7 represent a system of three nonlinear simultaneous equations in the unknowns  $a, b$  and  $c$ . Since the normal equations are nonlinear, their solution requires an iterative approach. It was found that the Secant Method (133) proved very successful in their solution.

APPENDIX JDESIGN OF DIGITAL FILTERS

Throughout the analysis procedures described in this project, extensive use has been made of digital filters. These filters have been used for a number of purposes including noise removal, the suppression of unwanted harmonics and the extraction of a particular frequency band from a signal. The three types of filters used are shown in idealised form in Figure J.1 and include low pass, band pass and band reject filters.

The general relationship between the input  $x(t)$  and the output  $y(t)$  of a linear filter is given by (5) the convolution integral

$$y(t) = \int_{-\infty}^{\infty} h(\tau) x(t - \tau) d\tau \quad (J.1)$$

where  $h(\tau)$  is the weighting function of the filter. The frequency response function or transfer function of the filter,  $H(f)$ , is the Fourier transform of  $h(\tau)$ , defined by

$$H(f) = \int_{-\infty}^{\infty} h(\tau) \exp(-i2\pi f\tau) d\tau \quad (J.2)$$

In designing a digital filter, unlike an analog filter, it is not necessary for the filter to be physically realizable. That is, it is not required that  $h(\tau)$  be zero for  $\tau < 0$ , since the data can be stored in the computer and then run backwards, to filter the data in reverse order.

The finite sum equivalent in Equation J.1 for  $t = k\Delta t$ ,  $k = 1, 2, \dots, M$ , can be expressed by a symmetric filter having the form

$$y_n = \sum_{k=-M}^M h_k x_{n-k} \quad , \quad n = 1, 2, \dots, N \quad (J.3)$$

where  $h_k = h_{-k}$ . Note that Equation J.3 involves future values of the input. Although this poses no problems in a digital sense, it again indicates that the filter is not physically realizable. For convenience, the sampling interval  $\Delta t$  is usually included in the filter weights. With a symmetric filter, the finite sum equivalent to Equation J.2 gives a filter with zero phase characteristics, namely

$$H(f) = \sum_{k=-M}^M h_k \cos(2\pi f k \Delta t) \quad (\text{J.4})$$

Equations J.3 and J.4 have a total of  $2M + 1$  coefficients  $h_k$ , known as filter weights. The  $k$ th weight is given by the inverse Fourier transform of Equation J.4 as (5)

$$h_k = \int_{-\infty}^{\infty} H(f) \cos(2\pi f k \Delta t) df \quad (\text{J.5})$$

Due to the symmetric nature of the filter and since the physically realistic limits of integration are zero and the Nyquist frequency  $f_N$ , Equation J.5 becomes

$$h_k = 2 \int_0^{f_N} H(f) \cos(2\pi f k \Delta t) df \quad (\text{J.6})$$

Filters of this type, whether symmetric or not, are called nonrecursive digital filters because their output is the result of a finite sum of input terms only. Using Equation J.6 it is possible to design any required filter simply by specifying  $H(f)$  and solving the integral. This is done below for the three specific filters used in this project.

(a) Low Pass Filter

An ideal low pass filter has a transfer function of the form

$$H(f) = \begin{cases} 1, & 0 \leq f \leq f_C \\ 0, & f_C < f < f_N \end{cases} \quad (\text{J.7})$$

where  $f_C$  is the cutoff frequency of the filter. Substituting Equation J.7 into J.6 gives

$$h_k = 2 \int_0^{f_C} \cos(2\pi f k \Delta t) df \quad (\text{J.8})$$

$$= \frac{\sin(2\pi f_C k \Delta t)}{\pi k \Delta t} \quad (\text{J.9})$$

Equation J.9 can also be expressed in terms of the sinc function, where  $\text{sinc}(x) = \sin x/x$ , as

$$h_k = 2 f_C \text{sinc}(2\pi f_C k \Delta t) \quad (\text{J.10})$$

Equation J.10 can introduce errors when used in Equation J.3 because of the finite number of filter weights  $M$ . These problems can be solved by noting that

$$2 f_C = \frac{1}{\int_{-\infty}^{\infty} \text{sinc}(2\pi f_C k \Delta t) dt} \quad (\text{J.11})$$

Replacing the integral in Equation J.11 with a summation and substituting in Equation J.10 yields

$$h_k = \frac{\text{sinc}(2\pi f_C k \Delta t)}{\sum_{j=-M}^M \text{sinc}(2\pi f_C j \Delta t) \Delta t} \quad (\text{J.12})$$

From Equation J.9 it can be seen that the filter weights are proportional to  $(1/k)$ , so that large values of  $k$  are required before these weights become small. In practice, this type of nonrecursive filter usually requires so many weights (100 or more) that it is not considered to be a very efficient method of filtering. In addition, if the number of filter weights is not large, truncation errors will occur between the desired  $H(f)$  and that found by the  $h_k$  weights. This is a result of the abrupt transition in  $H(f)$  from zero to one which causes a "Gibbs" phenomenon overshoot in the vicinity of the cutoff frequency. The transfer function of this low pass filter is shown for various numbers of filter weights in Figure J.2. It is clear from this figure that for 200 filter weights the transfer function is nearly ideal. Since computer resources were not at a premium, this form of filter was used with 200 filter weights.

(b) Band Pass Filter

The transfer function for an ideal band pass filter can be defined as

$$H(f) = \begin{cases} 0, & 0 \leq f < f_L \\ 1, & f_L \leq f \leq f_H \\ 0, & f_H < f \leq f_N \end{cases} \quad (\text{J.13})$$

where  $f_L$  and  $f_H$  are the low and high frequency limits of the pass band respectively. Substituting Equation J.13 into J.6 gives

$$h_f = 2 \int_{f_L}^{f_H} \cos(2\pi f k \Delta t) df \quad (\text{J.14})$$

which, upon integration, yields

$$h_k = \frac{\text{sinc}(2\pi f_H k \Delta t)}{\sum_{j=-M}^M \text{sinc}(2\pi f_H j \Delta t) \Delta t} - \frac{\text{sinc}(2\pi f_L k \Delta t)}{\sum_{j=-M}^M \text{sinc}(2\pi f_L j \Delta t) \Delta t} \quad (\text{J.15})$$

The transfer function for this band pass filter with  $f_L = 7.5$  Hz,  $f_H = 17.5$  Hz and  $M = 200$  is shown in Figure J.3. The very sharp cutoff characteristics and zero phase response are clearly evident in this figure. The phase relationship outside the pass band appears to be random. This, however, is purely a numerical round-off effect caused by the extremely small amount of energy left outside the pass band after filtering. Hence, the phase results for frequencies outside the pass band are of no significance.

(c) Band Reject Filter

The transfer function for an ideal band reject filter can be defined as

$$H(f) = \begin{cases} 1, & 0 \leq f \leq f_L \\ 0, & f_L < f < f_H \\ 1, & f_H \leq f \leq f_N \end{cases} \quad (\text{J.16})$$

where  $f_L$  and  $f_H$  are the low and high frequency limits of the reject band respectively. Substituting Equation I.16 into J.6 gives

$$h_k = \int_0^{f_L} \cos(2\pi f k \Delta t) dt + \int_0^{f_N} \cos(2\pi f k \Delta t) dt \quad (J.17)$$

which, upon integration yields

$$h_k = \frac{\text{sinc}(2\pi f_L k \Delta t)}{\sum_{k=-M}^M \text{sinc}(2\pi f_L k \Delta t) \Delta t} + \frac{\text{sinc}(2\pi f_N k \Delta t)}{\sum_{k=-M}^M \text{sinc}(2\pi f_N k \Delta t) \Delta t} - \frac{\text{sinc}(2\pi f_H k \Delta t)}{\sum_{k=-M}^M \text{sinc}(2\pi f_H k \Delta t) \Delta t} \quad (J.18)$$

The transfer function for this band reject filter with  $f_L = 7.5$  Hz,  $f_H = 17.5$  Hz and  $M = 200$  is shown in Figure J.4. The sharp cutoff characteristics and zero phase response of the filter can be clearly seen in this figure.

Whenever a nonrecursive filter of any of the designs discussed above is used,  $M$  points at the beginning and end of the time series must remain unfiltered. In the present project  $M = 200$  and, therefore, the first and last 200 points in any filtered time series were discarded.

## APPENDIX K

## RELATIONSHIP BETWEEN FIXED PROBE AND OSCILLATING PROBE MEASUREMENTS

The ultimate aim of the pressure and velocity measurements described in Chapter 7 and 8 was to determine the stress at the air-water interface. Since it is not possible to measure the stress exactly at the interface, it is necessary to determine the air flow quantities at various heights above the interface and then extrapolate the results to the water surface. In the fixed probe co-ordinate system, the elevation of the probe varies with the phase of the wave, thus complicating the extrapolation process. For the wave following probe, however, the probe elevation is constant with respect to the water surface, despite the wave phase.

If any external flow disturbances are neglected, the relationship between pressure and velocity fields in the oscillating and fixed frames of reference can be related by a simple co-ordinate transformation. The relationships between the two reference frames are

$$x = X; \quad z = Z + a \cos (\omega T); \quad t = T \quad (K.1)$$

where  $(x,z,t)$  and  $(X,Z,T)$  are the space and time co-ordinates in the fixed and moving frames respectively. Any function  $f(x,z,t)$  expressed in the fixed frame of reference can be described in terms of the moving co-ordinates by Equation K.1

$$f(x,z,t) = f[X(X,Z,T), z(X,Z,T), t(X,Z,T)] \quad (K.2)$$

Hence, the pressure and velocity fields, as measured in Chapter 7 and 8, will vary depending on the reference frame for the measurements.

BIBLIOGRAPHY

1. AMOROCHO, J. and DE VRIES, J.J., "A New Evaluation of the Wind Stress Coefficient Over Water Surfaces", *Jnl. Geophysical Research*, Vol. 85, No. C1, 1980, pp. 433-442., Comment by SMITH, S.D. and Reply, *Jnl. Geophysical Research*, Vol. 86, No. C5, 1981, pp. 4307-4308.
2. BANNER, M.L. and MELVILLE, W.K., "On the Separation of Air Flow Over Water Waves", *Jnl. Fluid Mechanics*, Vol. 77, No. 4, 1976, pp. 825-842.
3. BARNETT, T.P., "On the Generation, Dissipation, and Prediction of Ocean Wind Waves", *Jnl. Geophysical Research*, Vol. 73, No. 2, 1968, pp. 513-529.
4. BARNETT, T.P. and WILKERSON, J.C., "On the Generation of Ocean Wind Waves as Inferred by Airborne Radar Measurements of Fetch-Limited Spectra", *Jnl. Marine Research*, Vol. 25(3), 1967, pp. 292-328.
5. BENDAT, J.S. and PIERSON, A.G., "Random Data: Analysis and Measurement Procedures", Wiley, 1971, 407 pp.
6. BERGH, H. and TIJDEMAN, H., "Theoretical and Experimental Results for the Dynamic Response of Pressure Measuring Systems", National Aero and Astronautical Research Institute, Report No. NLR-TR-F.238, 1965, 19 pp.
7. BIESEL, F., "General 2nd Order Equations of Irregular Waves", *La Houille Blanche*, 7, 1952, pp. 372-376.
8. BIESEL, F. and SUQUET, F., "Laboratory Wave-Generating Apparatus", St. Anthony Falls Hydraulic Laboratory, University of Minnesota, Research Report No. 39, 1954, 133 pp.
9. BINGHAM, C., GODFREY, M.D. and TUKEY, J.W., "Modern Techniques of Power Spectrum Estimation", *Trans. IEEE Audio and Electroacoustics*, AU-15, June 1967.

10. BLACKMAN, R.B. and TUKEY, J.W., "The Measurement of Power Spectra", Dover, New York, 1958.
11. BOLE, B., "Wave Energy Transfer Mechanisms in Wind-Wave Tunnels", Jnl. Waterways, Harbors and Coastal Engineering Div., ASCE, WW4, Nov. 1974, pp. 325-344.
12. BOLE, J.B. and HARRIS, D.L., "Considerations for a CERC Laboratory Wind-Wave Research Program", Submitted to CERC, Sept. 1973, 68 pp.
13. BRADSHAW, P., "An Introduction to Turbulence and its Measurement", Pergamon Press, 1975, 218 pp.
14. BROCKS, K., "Ein Neues Gerat fur Störungsfreie Meteorologische Messungen auf dem Meer", Arch. Met. Geophys. Biokl. A, 11, 1959, pp. 227-239.
15. BROOKE BENJAMIN, T., "Shearing Flow Over a Wavy Boundary", Jnl. Fluid Mechanics, Vol. 6, 1959, pp. 161-205.
16. BRYER, D.W. and PANKHURST, R.C., "Pressure-Probe Methods for Determining Wind Speed and Flow Directions", Her Majesty's Stationery Office, London, 1971, 125 pp.
17. CARDONE, V.J., PIERSON, W.J. and WARD, E.G., "Hindcasting the Directional Spectra of Hurricane-Generated Waves", Jnl. Petroleum Technology, AIIME, 261, 1976, pp. 385-394.
18. CERMAK, J.E., "Laboratory Simulation of the Atmospheric Boundary Layer", AIAA Journal, Vol. 9, No. 9, Sept. 1971, pp. 1746-1754.
19. CERMAK, J.E., "Applications of Fluid Mechanics to Wind Engineering - A Freeman Scholar Lecture", Jnl. of Fluids Engineering, March 1975, pp. 9-38.
20. CHAMPAGNE, F.H., SCHLEICHER, C.A. and WEHRMANN, O.H., "Turbulence Measurements with Inclined Hot-Wires, Parts 1 and 2", Jnl. Fluid Mechanics, Vol. 28, 1967, pp. 153-175.

21. CHAO, S.P. and HSU, E.Y., "Wave-Induced Velocities and Turbulent Reynolds Stress Above an Air-Water Interface", *Dynamics of Atmospheres and Oceans*, 2, 1978, pp. 471-493.
22. CORRSIN, S., "Turbulence: Experimental Methods", *Handbuch der Physik*, Vol. 8, Part 2, Springer, 1963.
23. DAVENPORT, A.G., "The Relationship of Wind Structure to Wind Loading", *Proc. of Conference on Building and Structures*, National Physical Laboratory, Great Britain, 1963, pp. 54-83.
24. DAVIES, P., and MASON, J., "The I.S.V.R. Constant Temperature Hot Wire Anemometer", *ISVR Tech. Report No. 66*, University of Southampton, 1974, 31 pp.
25. DAVIS, R.E., "On Prediction of the Turbulent Flow Over a Wavy Boundary", *Jnl. Fluid Mechanics*, Vol. 52, 1972, pp. 287-306.
26. DOBSON, F.W., "Observations of Normal Pressure on Wind-Generated Sea Waves", *Ph.D. Dissertation*, Institute of Oceanography, University of British Columbia, 1969.
27. DOBSON, F.W., "Measurements of Atmospheric Pressure on Wind-Generated Sea Waves", *Jnl. Fluid Mechanics*, Vol. 48, 1971, pp. 91-127.
28. ELLIOTT, J.A., "Microscale Pressure Fluctuations Measured Within the Lower Atmospheric Boundary Layer", *Jnl. Fluid Mechanics*, Vol. 53, 1972, pp. 353-383.
29. ELLIOTT, J.A., "Microscale Pressure Fluctuations Near Waves being Generated by Wind", *Jnl. Fluid Mechanics*, Vol. 54, 1972, pp. 427-448.
30. EWING, J.A., "A Numerical Wave Prediction for the North Atlantic Ocean", *Deutsche Hydrographische Zeitschrift*, Jahrgang 24, Heft 5, 1971, pp. 241-261.
31. FORRISTALL, G.Z., REECE, A.M., THRO, M.E., WARD, E.G., DOYLE, E.H. and HAMILTON, R.C., "Measurements of Sea Wave Attenuation Due to Deformable Bottoms", *ASCE Fall Convention*, October 1980.

32. FOX, M.J.H., "On the Nonlinear Transfer of Energy in the Peak of a Gravity-Wave Spectrum", Proc. Royal Society A, 348, 1976, pp. 467-483.
33. FRIEHE, C.A. and SCHWARTZ, W.H., "Deviation from the Cosine Law For Yawed Cylindrical Anemometer Sensors", Trans. A.S.M.E., 35E, 1968, pp. 655-
34. GARRETT, C. and SMITH, J., "On the Interaction Between Long and Short Surface Waves", Jnl. Physical Oceanography, Vol. 6(6), 1976, pp. 925-930.
35. GELCI, R., CAZALE, J. and VASSAL, J., "Utilization des Diagrams de Propagation a la Provision Energitique de le Houle", Bulletin d'Information du Commite Central d'Oceanographic et d'Etude des Cotes, VIII, No. 4, 1956, pp. 169-187.
36. GENT, P.R. and TAYLOR, P.A., "A Numerical Model of Air Flow Above Water Waves", Jnl. Fluid Mechanics, Vol. 77, 1976, pp. 105-128.
37. GOLDSTEIN, S., "A Note on the Measurement of Total Head and Static Pressure in a Turbulent Stream", Proc. Royal Society A, 155, 1936, pp. 570-
38. HASSELMANN, K., "On the Nonlinear Energy Transfer in a Gravity Wave Spectrum, Part 1, General Theory", Jnl. Fluid Mechanics, Vol. 12, 1962, pp. 481-500.
39. HASSELMANN, K., "On the Nonlinear Energy Transfer in a Gravity Wave Spectrum, Part 2, Conservation Theorems; Wave-Particle Analogy; Irreversibility", Jnl. Fluid Mechanics, Vol. 15, 1963, pp. 372-281.
40. HASSELMANN, K., "On the Nonlinear Energy Transfer in a Gravity Wave Spectrum, Part 3, Evaluation of the Energy Flux for a Swell-Sea Interaction for a Neumann Spectrum", Jnl. Fluid Mechanics, Vol. 15, 1963, pp. 385-398.
41. HASSELMANN, K., "Basic Developments in Fluid Dynamics Vol. 2", M. Holt (Ed.), Academic Press, 1968, pp. 117-182.

42. HASSELMANN, K., "On the Mass and Momentum Transfer Between Short Gravity Waves and Larger-Scale Motions", *Jnl. Fluid Mechanics*, Vol. 50, 1971, pp. 189-205.
43. HASSELMANN, K. and COLLINS, J.I., "Spectral Dissipation of Finite-Depth Gravity Waves due to Turbulent Bottom Friction", *Jnl. Marine Research*, 26, 1968, pp. 1-12.
44. HASSELMANN, S. and HASSELMANN, K., "A Symmetric Method of Computing the Nonlinear Transfer in a Gravity Wave Spectrum", *Hamburger Geophysikalische Einzelschriften, Reihe A*, 52, 1981, 173 pp.
45. HASSELMANN, K., et al., "Measurements of Wind-Wave Growth and Swell Decay during the Joint North Sea Wave Project (JONSWAP)", *Deutsches Hydrographisches Institut, Hamburg*, 1973, 95 pp.
46. HASSELMANN, K., "A Parametric Wave Prediction Model", *Jnl. Physical Oceanography*, Vol. 6, No. 2, 1976, pp. 200-228.
47. HELMHOLTZ, H., "On Discontinuous Movements of Fluids", *Trans. by F. Guthrie, Philos. Mag.*, 36, pp. 337-348.
48. HSIAO, S.V. and SHEMDIN, O.H., "Interaction of Ocean Waves with a Soft Bottom", *Jnl. Physical Oceanography*, Vol. 10, No. 4, April 1980, pp. 605-610.
49. HUNT, J.N., "Viscous Damping of Waves over an Inclined Bed in a Channel of Finite Width", *Houille Blanche*, Vol. 7, 1952, pp. 836-842.
50. HSU, C.T., HSU, E.Y. and STREET, R.L., "On the Structure of Turbulent Flow over Progressive Water Waves: Theory and Experiment in a Transformed Wave-Following Co-ordinate System", *Jnl. Fluid Mechanics*, Vol. 105, 1981, pp. 87-117.
51. IWASAKI, T. and SATO, M., "Dissipation of Wave Energy Due to Opposing Current", *12th International Coastal Engineering Conference, Vancouver, Canada*, 1972, pp. 605-622.

52. JEFFREYS, H., "On the Formation of Water Waves by Wind", Proc. Royal Society, London, A, Vol. 107, 1925, pp. 189-206.
53. JONSSON, I.G., "Friction Factor Diagrams for Oscillatory Boundary Layers", Progress Report, Technical University, Denmark, No. 10, 1965, pp. 10-21.
54. KAMPHUIS, J.W., "Scale Selection for Wave Models", C.E. Research Report No. 71, Dept. Civil Engineering, Queen's University, Kingston, Ontario, Canada, 1972, 85 pp.
55. KEATING, T. and WEBBER, N.B., "Generation of Periodic Waves in a Laboratory Channel: A Comparison Between Theory and Experiment", Proc. Institution of Civil Engineers, 2, 63, 1977, pp. 819-832.
56. KELVIN, LORD, W., "The Influence of Wind on Waves in Water Supposed Frictionless", Philos. Mag., 10, 1871, pp. 92-100.
57. KENDALL, J.M., "The Turbulent Boundary Layer Over a Wall with Progressive Surface Waves", Jnl. Fluid Mechanics, Vol. 41, 1970, pp. 259-281.
58. KEULEGAN, G., "Wind Tides in Small Closed Channels", N.B.S. Research Paper No. 2207, 1951.
59. KING, D.B. and SHEMDIN, O.H., "Radar Observations of Hurricane Wave Direction", Proc. 16th International Conference on Coastal Engineering, Hamburg, West Germany, 1978.
60. KINSMAN, B., "Wind-Waves", Prentice-Hall, Englewood-Cliffs, New Jersey, 1965, 675 pp.
61. KITAIGORODSKII, S.A., "The Physics of Air-Sea Interaction", NTIS, TT 72-50062, 1970, 237 pp.
62. KITAIGORODSKII, S.A., KRASITSKII, V.P. and ZASLAVSKII, M.M., "On Phillips' Theory of Equilibrium Range in the Spectra of Wind-Generated Gravity Waves", Jnl. Physical Oceanography, 5, 1875, pp. 410-420.

63. KLINE, S.J. and McCLINTOCK, F.A., "Describing Uncertainties in Single-Sample Experiments", Mechanical Engineering, January 1953, pp. 3-8.
64. LAI, R.J. and SHEMDIN, O.H., "Laboratory Investigation of Air Turbulence above Simple Water Waves", Jnl. Geophysical Research, Vol. 76, No. 30, 1971, pp. 7334-7350.
65. LAMB, H., "Hydrodynamics", Cambridge University Press, 1932, 738 pp.
66. LE BLOND, P.H. and MYSAK, L.A., "Waves in the Ocean", Elsevier, 1978, 602 pp.
67. LE MEHAUTE, B., "An Introduction to Hydrodynamics and Water Waves, Volume I: Fundamentals", ESSA Tech. Report No. ERL 118-POL 3-1, 1969, 503 pp.
68. LILLY, D.K., Appendix: "On the Speed of Surface Gravity Waves Propagating on a Moving Fluid", from Hidy, G.M. and Plate, E.J., "Wind Action on Water Standing in a Laboratory Channel", Jnl. Fluid Mechanics, Vol. 26, 1966, pp. 651-687.
69. LONG, R.B., "Scattering of Surface Waves by an Irregular Bottom", Jnl. Geophysical Research, Volume 78, No. 33, 1973, pp. 7861-7870.
70. LONGUET-HIGGINS, M.S., "On the Transformation of a Continuous Spectrum by Refraction", Proc. Cambridge Phil. Soc., 53, 1957, pp. 226-229.
71. LONGUET-HIGGINS, M.S., "Action of a Variable Stress at the Surface of Water Waves", Physics of Fluids, Vol. 12, No. 4, 1969, pp. 737-740.
72. LONGUET-HIGGINS, M.S. "A Nonlinear Mechanism for the Generation of Sea Waves", Proc. Royal Society, London, A, 311, 1969, pp. 371-389.
73. LONGUET-HIGGINS, M.S., "On the Nonlinear Transfer of Energy in the Peak of a Gravity-Wave Spectrum: A Simplified Model", Proc. Royal Society, A, 347, 1976, pp. 311-328.

74. LONGUET-HIGGINS, M.S., CARTWRIGHT, D.E. and SMITH, N.D., "Observations of the Directional Spectrum of Sea Waves Using the Motions of a Floating Buoy", In: "Ocean Wave Spectra", Prentice Hall, 1963, pp. 111-136.
75. LONGUET-HIGGINS, M.S. and STEWART, R.W., "Changes in the Form of Short Gravity Waves and Long Waves and Tidal Currents", Jnl. Fluid Mechanics, Vol. 8, 1960, pp. 565-583.
76. LONGUET-HIGGINS, M.S. and STEWART, R.W., "The Change in Amplitude of Short Gravity Waves on Steady Non-Uniform Currents", Jnl. Fluid Mechanics, Vol. 10, 1961, pp. 529-549.
77. MADSEN, O.S., "On the Generation of Long Waves", Jnl. Geophysical Research, Vol. 76, 1971, pp. 8672-8683.
78. MILES, J.W., "On the Generation of Surface Waves by Shear Flows", Jnl. Fluid Mechanics, Vol. 3, 1957, pp. 185-204.
79. MILES, J.W., "On the Generation of Surface Waves by Shear Flows, Part 2", Jnl. Fluid Mechanics, Vol. 6, 1959, pp. 568-582.
80. MILES, J.W., "On the Generation of Surface Waves by Turbulent Shear Flows", Jnl. Fluid Mechanics, Vol. 7, 1960, pp. 469-478.
81. MILES, J.W., "On the Generation of Surface Waves by Shear Flows, Part 4", Jnl. Fluid Mechanics, Vol. 13, 1962, pp. 433-448.
82. MILES, J.W., "On the Generation of Surface Waves by Shear Flows, Part 5", Jnl. Fluid Mechanics, Vol. 30, 1967, pp. 163-175.
83. MITCHELL, G.M., SOBEY, R.J., BARBAGALLO, A.M.J. and COLMAN, E.J., "A Programmable Water Wave Generator", Research Bull. No. CS18, Dept. Civil and Systems Eng., James Cook University, Townsville, Australia, 1979, 105 pp.
84. MORRISON, J.L.M. and CROSSLAND, B., "An Introduction to the Mechanics of Machines", Longman, 1971, 461 pp.

85. MUNK, W.H. and ARTHUR, R.S., "Wave Intensity Along a Refracted Ray", Gravity Waves, U.S. National Bureau of Standards, Circular 521, 1952, pp. 95-108.
86. OTNES, R.K. and ENOCHSON, L., "Digital Time Series Analysis", Wiley, 1972, 467 pp.
87. OTNES, R.K. and ENOCHSON, L., "Applied Time Series Analysis, Volume I: Basic Techniques", Wiley, 1978, 449 pp.
88. PANKHURST, R.C. and HOLDER, D.W., "Wind-tunnel Techniques", Pitman, London, 1965, 702 pp.
89. PHILLIPS, O.M., "On the Generation of Waves by Turbulent Wind", Jnl. Fluid Mechanics, Vol. 2, 1957, pp. 417-445.
90. PHILLIPS, O.M., "The Equilibrium Range in the Spectrum of Wind Generated Waves", Jnl. Fluid Mechanics, Vol. 4, 1958, pp. 426-434.
91. PHILLIPS, O.M., "On the Dynamics of Unsteady Gravity Waves of Finite Amplitude, Part I", Jnl. Fluid Mechanics, Vol. 9, 1960, pp. 193-217.
92. PHILLIPS, O.M., "On the Attenuation of Long Gravity Waves by Short Breaking Waves", Jnl. Fluid Mechanics, Vol. 16, 1963, pp. 321-332.
93. PHILLIPS, O.M., "The Dynamics of the Upper Ocean", 1st Edition, Cambridge Univ. Press, 1966, 261 pp.
94. PHILLIPS, O.M., "The Dynamics of the Upper Ocean", 2nd Edition, Cambridge Univ. Press, 1977, 336 pp.
95. PHOENIX Centrifugal Fan Catalogue, Catalogue No. ALA 3-74, 1974, 75 pp.
96. PIERSON, W.J., TICK, L.J. and BAER, L., "Computer-Based Procedures for Predicting Global Wave Forecasts and Wind Field Analyses Capable of Using Wave Data Obtained by a Spacecraft", Proc. 6th Naval Hydrodynamics Symposium, Vol. 2, 1966.

97. PLATE, E.J., "Aerodynamic Characteristics of Atmospheric Boundary Layers", U.S. Atomic Energy Commission, NTIS, No. TID-25465, 1971, 190 pp.
98. PLATE, E.J., CHANG, P.C. and HIDY, G.M., "Experiments on the Generation of Small Water Waves by Wind", Jnl. Fluid Mechanics, Vol. 35, 1969, pp. 625-656.
99. PLATE, E.J. and NATH, J.H., "Modelling of Structures Subjected to Wind Generated Waves", Proc. 11th Conference on Coastal Engineering, Vol. 2, 1968, pp. 745-760.
100. POPE, A. and HARPER, J.J., "Low-Speed Wind Tunnel Testing", Wiley, 1966.
101. PRIESTLEY, J.T., "Correlation Studies of Pressure Fluctuations on the Ground Beneath a Turbulent Boundary Layer", National Bureau of Standards, Report 8942, Project 21301-20-2130400, 1965.
102. PUTNAM, J.A., "Loss of Wave Energy Due to Percolation in a Permeable Sea Bottom", Transactions of the American Geophysical Union, Vol. 30, No. 3, 1949, pp. 349-357.
103. RICHTER, K., SCHMALFELDT, B. and SIEBERT, J., "Bottom Irregularities in the North Sea", Deutsche Hydrogr. Zeits., 29, 1976, pp. 1-10.
104. ROLL, H.U., "Wassernahes Windprofil und Wellen auf dem Wattenmeer", Ann. Met., 1, 1948, pp. 139-151.
105. SCHLICHTING, H., "Boundary-Layer Theory", 6th Edition, McGraw-Hill, 1968.
106. SELL, W. and HASSELMANN, K., "Computations of Nonlinear Energy Transfer for JONSWAP and Empirical Wind Wave Spectra", Rep. Inst. Geophys., University Hamburg, 1972.
107. SHAW, R., "The Measurement of Static Pressure", Jnl. Fluid Mechanics, Vol. 7, 1960, pp. 550-

108. SHEMDIN, O.H., "Instantaneous Velocity and Pressure Measurements Above Propagating Waves", Tech. Report No. 4, Dept. of Coastal and Oceanographic Eng., Univ. of Florida, 1969, 105 pp.
109. SHEMDIN, O.H., "Momentum Transfer at the Air-Water Interface", American Institute of Chemical Engineers, Symposium on Transport Processes in Lakes and Oceans, Atlantic City, 1967, pp. 263-284.
110. SHEMDIN, O.H., HASSELMANN, K., HSIAO, S.V. and HERTEICH, K., "Nonlinear and Linear Bottom Interaction Effects in Shallow Water", In Favre, A. and Hasselman, K. (eds.), "Turbulent Fluxes Through the Sea Surface, Wave Dynamics, and Prediction", Plenum Press, 1977, pp. 347-372.
111. SHEMDIN, O.H. and HSU, E.Y., "The Dynamics of Wind in the Vicinity of Progressive Water Waves", Jnl. Fluid Mechanics, Vol. 30, 1967, pp. 403-416.
112. SHEMDIN, O.H. and TOBER, G., "Surface Followers", In "Air-Sea Interaction", edited by Dobson, F., Hasse, L. and Davis, R., Plenum Press, 1980, pp. 627-644.
113. SIMIU, E. and SCANLAN, R.H., "Wind Effects on Structures: An Introduction to Wind Engineering", Wiley, 1978.
114. SNODGRASS, F.E., et al., "Propagation of Ocean Swell Across the Pacific", Phil. Trans. Royal Society, London, A, 259, 1966, pp. 431-497.
115. SNYDER, R.L., "A Field Study of Wave-Induced Pressure Fluctuations Above Surface Gravity Waves", Jnl. Marine Research, 32, 1974, pp. 485-496.
116. SNYDER, R.L. and COX, C.S., "A Field Study of the Wind Generation of Ocean Waves", Jnl. Marine Research, Vol. 24, 2, 1966, pp. 141-178.
117. SNYDER, R.L., DOBSON, F.W., ELLIOTT, J.A. and LONG, R.B., "Array Measurements of Atmospheric Pressure Fluctuations Above Surface Gravity Waves", Jnl. Fluid Mechanics, Vol. 102, 1981, pp. 1-59.

118. SOBEY, R.J., "Numerical Alternatives in Transient Stream Response", to appear in, Jnl. Hydraulic Engineering, ASCE, Vol. 109, 1983.
119. SOBEY, R.J. and COLMAN, E.J., "Natural Wave Trains and Scattering Transform", ASCE, Jnl. Waterway, Port, Coastal and Ocean Div., Vol. 108, No. WW3, 1982.
120. SOBEY, R.J. and YOUNG, I.R., "A Spectral Model of Tropical Cyclone Wind Waves", submitted to Quarterly Jnl. Royal Met. Society.
121. STANDARDS ASSOCIATION OF AUSTRALIA, "S.A.A. Loading Code, Part 2 - Wind Forces", AS1170, Part 2, 1973.
122. STANTON, T., "The Growth of Waves on Water Due to the Action of Wind", Proc. Royal Society, A, 137, 1937, pp. 283-292.
123. STEWART, R.H., "Laboratory Studies of the Velocity Field Over Deep-Water Waves", Jnl. Fluid Mechanics, Vol. 42, 1970, pp. 733-754.
124. STEWART, R.H. and TEAGUE, C., "Dekameter Radar Observations of Ocean Wave Growth and Decay", Jnl. Physical Oceanography, Vol. 10, No. 1, 1980, pp. 128-143.
125. STOKES, G.G., "On the Theory of Oscillatory Waves", Trans. Cambridge Philos. Soc., 8, 1847, pp. 441-455.
126. TAKEDA, A., "Wind Profiles Over Sea Waves", Jnl. Ocean Soc. Japan, 19, 1963, pp. 16-22.
127. TAKEUCHI, K., LEAVITT, E. and CHAO, S.P., "Effects of Water Waves on the Structure of Turbulent Shear Flow", Jnl. Fluid Mechanics, Vol. 80, 1977, pp. 535-559.
128. TAYLOR, G.I., "An Experimental Study of Standing Waves", Proc. Royal Society, A, 223, 1953, pp. 446-468.
129. URSELL, F., "Wave Generation by Wind", In "Survey in Mechanics", London: Cambridge University Press, 1956, pp. 216-249.

130. URSELL, F., DEAN, R.G. and YU, Y.S., "Forced Small Amplitude Water Waves: A Comparison of Theory and Experiment", Jnl. Fluid Mechanics, Vol. 7, 1960, pp. 33-52.
131. VAN DORN, W.G., "Wind Stress on an Artificial Pond", Jnl. Marine Research, Vol. 12, 1953, pp. 249-276.
132. WALPOLE, R.E. and MYERS, R.H., "Probability and Statistics for Engineers and Scientists", MacMillan, 1972, 506 pp.
133. WOLFE, P., "The Secant Method for Simultaneous Non-Linear Equations", Communications of the ACM, Vol. 2, 1959.
134. WU, H.Y., HSU, E.Y. and STREET, R.L., "The Energy Transfer Due to Air-Input, Non-Linear Wave-Wave Interaction and White-Cap Dissipation Associated with Wind-Generated Waves", Dept. Civil Eng., Stanford University, Tech. Rep. No. 207, 1977, 158 pp.
135. YALIN, M.S., "Theory of Hydraulic Models", Chapter 7, Waves, MacMillan Press, 1971.
136. YOUNG, I.R. and SOBEY, R.J., "The Numerical Prediction of Tropical Cyclone Wind-Waves", Research Bull. No. CS20, Dept. of Civil and Systems Eng., James Cook University, Townsville, Australia, 1981, 378 pp.
137. YU, H. and LIN, J., "A Technique for Generating a Turbulent Boundary Layer in a Wind-Wave Tank", Proc., 2nd., U.S. National Conference on Wind Engineering Research, Colorado State Univ., June 1975.
138. SAVILLE, T., JR., "Wind Setup and Waves in Shallow Water", TM-27, U.S. Army, Corps of Engineers, Beach Erosion Board, Washington, D.C., June 1952.
139. SOBEY, R.J., HARPER, B.A. and STARK, K.P., "Numerical Simulation of Tropical Cyclone Storm Surge", Res. Bull. No. CS14, Dept. Civil and Systems Eng., James Cook Univ., Australia, 1977.

140. CROMIBE, D.S., et al., "H.F. Radar Observations of Sea Waves Travelling in Opposition to the Wind", *Boundary Layer Met.*, 13, 1978, pp 45-54.
141. DOBSON, F.W., "The Damping of a Group of Sea Waves", *Boundary Layer Met.*, 1, 1971, pp 399-410.
142. WRIGHT, J.W., "The Wind Drift and Wave Breaking", *Jnl. Phys. Ocean*, 6, 1976, pp 402-405.